Valence-band Auger line shapes for Si surfaces: Simplified theory and corrected numerical results*

Peter J. Feibelman and E. J. McGuire
Sandia Laboratories, Albuquerque, New Mexico 87115
(Received 9 August 1977)

A reduced version of the independent-electron theory of Auger line shapes is given that takes advantage of the general smallness of those components of a solid's local density of states (LDOS) matrix which are off-diagonal in angular momentum. Thus we present approximate formulae which relate the valence-band Auger line shapes of a solid simply to its angular-momentum projected LDOS near a surface. Using these simplified formulae, we have located and corrected a number of numerical errors in our previous calculations of the Auger line shapes of Si. We present corrected results here, showing that the independent-electron theory, coupled with the use of atomic Auger matrix elements for Si, actually predicts too large a probability of $L_{2,3}M_1M_{2,3}$ decay relative to that for $L_{2,3}M_{2,3}M_{2,3}$ decay to give good agreement with measured Si $L_{2,3}VV$ Auger line shapes. Possible reasons for the experimental smallness of the $L_{2,3}M_1M_{2,3}$ Auger decay rate are discussed. The Si $L_1L_{2,3}V$ Coster-Kronig line is also recalculated and shown to be in correspondence with the simplified theory of Auger transitions.

In a recent paper,[1] we have, with K. C. Pandey, presented numerical results for the valence-band Auger lines shapes of clean, ideal Si surfaces. In the course of generalizing our computer codes to permit similar calculations for more complicated surfaces, we have, however, uncovered a number of computation errors in our earlier work. The discovery of these errors raises a question which is important in its own right, namely, how are we to decide when the results of the rather complicated FORTRAN program written to evaluate Eqs. (2.15) and (2.25) of Ref. 1 are sensible; or more specifically, how can we develop a simple approximation to the line-shape theory of Ref. 1 which preserves the most important qualitative features of the full theory's predictions and thereby makes it easier to understand what underlies these features. The present note is accordingly intended to fulfill two purposes. First, it is in the nature of an erratum; i.e., we present corrected numerical results for the $L_{2,3}VV$ and $L_1L_{2,3}V$ Auger lines of Si surfaces. Second, it encompasses the development of a reduced version of the line-shape theory of Ref. 1, in which we take advantage of the fact that in general the diagonal components of the occupied local density-of-states matrix $F_{L,L'}(E,Z)$ [see Ref. 1, Eq. (2.16)] are considerably larger than the off-diagonal ones. This reduced line-shape theory points to a rather simple way of parametrizing Auger line-shape data. It also enables us to show that our corrected computer codes are now giving reasonable results.

The discussion which follows is divided into two parts, the first concerning the $L_{2,3}VV$ transition and the second, the $L_1L_{2,3}V$ Coster-Kronig decays. For the $L_{2,3}VV$ case we show that, to quite an accurate approximation, the theoretical line shapes are simply linear combinations of folds of the s-like and p-like local densities of states (LDOS's) on the Si atoms near a surface. With matrix elements calculated using atomic wave functions, the contributions of the cross-fold of the s- and p-like LDOS's turn out to be too large by a factor at least ~2 to give good agreement with experiment, contrary to our earlier finding.[1] We are therefore led to discuss the question of why these contributions might be smaller if we used Wannier rather than atomic orbitals to calculate Auger matrix elements.

In the case of the $L_1L_{2,3}V$ lines we show that again to a good approximation the theoretical line shape is a linear combination of contributions from the s- and p-like DOS's. Although we do present corrected numerical results here too, our qualitative conclusions concerning the comparison of theory and experiment are the same as they were in Ref. 1:

(i) The atomically calculated matrix elements overestimate the contribution of s electrons to the $L_1L_{2,3}V$ line shapes considerably; the matrix elements involving $3s$ electrons are a factor ~2.5 too large relative to those involving $3p$ electrons.

(ii) For the Si(111) surface the predicted line shape is too narrow by $\gtrsim$1 eV, as one can see by convolving the Si DOS and a Lorentzian of width ~1 eV, which is a reasonable guess[2] for the width of the Si $2s$ level, and comparing it to the data.

(iii) For the Si(100) surface our model, which does not incorporate the observed 2×1 reconstruction, shows substantial contributions due to back- and dangling-bond surface states. These features are not present in the data, presumably because

they are removed when the 2×1 reconstruction occurs.

$L_{2,3}VV$ LINES

The most significant error we have discovered is for this case. Due to faulty computer logic, the contributions of Auger decays involving one valence s electron and one valence p electron were deemphasized, ironically leading to excellent agreement with the data of Houston, Lagally, and Moore.[3] Now, as is shown in Fig. 1, we find that ratio of the radial matrix elements $\mathcal{R}_0(1111)$ and $\mathcal{R}_0(0110)$ [Ref. 1, Eq. (3.6)], which represent, respectively, the most important amplitudes for decays involving two $3p$ electrons and one $3p$ and one $3s$ electron, is too small by a factor $\gtrsim1.4$ to give good agreement with the data. We must therefore seek to understand why the calculation of this ratio using atomic wave functions underestimates its value. This question is discussed further below. First we wish to present a reduced

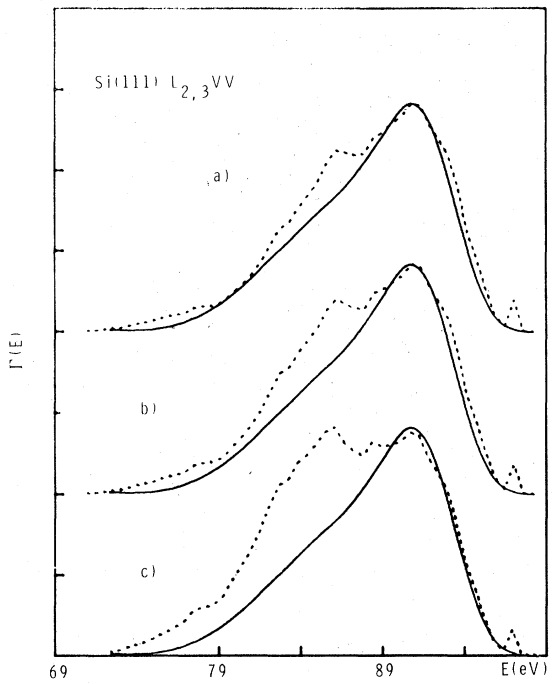

FIG. 1. Comparison of theoretical $L_{2,3}$ VV Auger line shapes for an ideal Si(111) surface, and data of Houston *et al.* (Ref. 3), solid curves. The theoretical (dotted) curve of (c) corresponds to the use of the atomically calculated matrix elements and phase shifts, given in Table I. The theoretical (dotted) curves (a) and (b) correspond to the use of the same atomic parameters except that the matrix element $\mathcal{R}_0(0110)$ is multiplied by $1/\sqrt{3}$ in the curve (a) and $1/\sqrt{2}$ in curve (b). For all the theoretical curves the inelastic mean free path was taken to be 7 Å.

version of the line-shape theory of Ref. 1, that shows that the ratio $\mathcal{R}_0(1111)/\mathcal{R}_0(0110)$ is in fact the crucial quantity and also shows that our present computer results are reasonable.

To begin we recall Eq. (2.15) of Ref. 1,[4]

$$\Gamma(E_f,Z)=\sum_{L_1,L_2,L_1',L_2'}\int d\omega\, F_{L_1,L_1'}(E_f-\omega,Z)\times F_{L_2,L_2'}(E_c+\omega,Z)\times W_{L_1,L_1',L_2,L_2'}(E_f,Z)\,, \tag{1}$$

which expresses the partial width $\Gamma(E_f,Z)$ for the Auger decay of a core hole of energy E_c in an atom at depth Z in terms of the local, occupied density-of-states matrix $F_{L,L'}(E,Z)$, where the angular-momentum index $L=(l,m)$, and where $W_{L_1,L_1',L_2,L_2'}$ is a rather complicated expression involving Auger matrix elements and geometric factors [cf., Ref. 1, Eq. (2.25)].

The main problem in analyzing Eq. (1) is that there are many terms in the sum, and most of them involve off-diagonal components of $F_{L,L'}(E,Z)$ which are not quantities for which one has much intuition. However, as is seen in Fig. 2, the only off-diagonal component of $F_{L,L'}(E,Z)$ which can be nonzero for Si(111), given the high degree of symmetry of this surface, is small in magnitude compared to the diagonal components despite the fact that sp^3 bonding is highly nonspherical. This result follows from the fact that the sp^3 bonds in Si are largely mixtures of s and p orbitals from *different* bands. Only for surface bands, which are narrow in energy and which tend to be located in small regions of the surface Brillouin zone should one thus expect substantial values of off-diagonal $F_{L,L'}$ components.

The generality of the smallness of the off-diagonal $F_{L,L'}$'s, coupled with the fact that, while the diagonal components of $F_{L,L'}$ are necessarily real and positive, the off-diagonal ones are complex (and should therefore contribute terms to Auger line shapes which tend to cancel because of phase randomness), permits us to reduce Eq. (1) to a much simpler though still fairly accurate form. We proceed by defining

$$\rho_L(E,Z)=F_{L,L}(E,Z) \tag{2}$$

and

$$f\otimes g\equiv\int d\omega\, f(E-\omega)g(E_c+\omega)\,. \tag{3}$$

Noting the identity,

$$f\otimes g\equiv g\otimes f\,, \tag{4}$$

we then rewrite Eq. (1) in the form

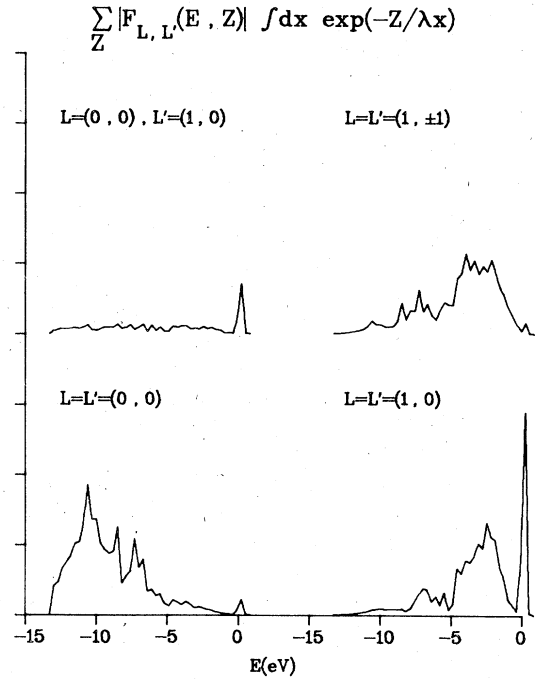

FIG. 2. Comparison of the magnitudes of the various components of the local-density-of-states matrix of a Si(111) surface. Each curve is labelled above by $L = (l, m)$ and $L' = (l', m')$ and represents the quantity,

$$\sum_j |F_{L,L'}(E, Z_j)| \int_0^1 dx \exp(-Z_j/\lambda x),$$

versus energy E, where Z_j is the depth of the jth layer and λ is the inelastic mean free path, taken to equal 7 Å. The only off-diagonal $F_{L,L'}$ which is nonzero for Si(111) is $F_{(0,0),(1,0)}$, because this surface has a threefold rotation axis and three mirror planes. [For Si(100), $F_{(1,1),(1,-1)}$ is also nonvanishing and for Si(110), none of the $F_{L,L'}$ vanishes identically.] The energies on the x axis are measured from the valence-band maximum. All curves are drawn to the same scale.

$$\Gamma(E_f, Z) = \sum_{L,L'} \rho_L \otimes \rho_{L'} W_{L,L,L',L'}(E_f, Z) + \sum_{\substack{L,L',L'' \\ L' \neq L''}} 2\,\rho_L \otimes F_{L'L''} W_{L,L,L',L''}(E_f, Z) + \sum_{\substack{L_1,L_1',L_2,L_2' \\ L_1,L_2 \neq L_1',L_2'}} F_{L_1,L_1'} \otimes F_{L_2,L_2'} \times W_{L_1,L_1',L_2,L_2'}(E_f, Z). \quad (5)$$

The interesting feature of Eq. (5) is that most of the terms in the second summation on the right-hand side are forced to vanish via angular-momentum selection rules. Thus the corrections to the first term of Eq. (5) are mostly quadratic in the off-diagonal F's and are therefore quite unimportant. In order to see why most of the terms in Eq. (5) that are linear in $F_{L',L''}$, $L' \neq L''$ vanish, note that the quantity $W_{L_1,L_1,L_2,L_2'}(E_f, Z)$ [Ref. 1, Eq. (2.25)] is a sum of products of Auger matrix elements of the form

$$M_{l_f,m_f;l_i,m_i;L_1,L_2} M^*_{l_{f2},m_f;l_i,m_i;L_1',L_2'}. \quad (6)$$

The quantum number m_i represents the orientation of the angular momentum of the decaying hole and thus is the same in both the M and the M^* factors. The quantum number m_f represents the orientation of the final Auger electron momentum. It is the same in both M and M^* because we assume that Auger electrons are collected over all 2π of azimuth angles. Finally if we are looking at terms in which $L_1 = L_1'$ then by definition $m_1 = m_1'$. Thus since the M's are *atomic* matrix elements: i.e., they are calculated for a central potential, conservation of angular momentum requires that $m_2 = m_2'$. Moreover this same argument applies to terms in W of the form

$$M_{l_{f1},m_f;l_i,m_i;L_1,L_2} M^*_{l_{f2},m_f;l_i,m_i;L_2',L_1'}. \quad (7)$$

Having concluded that in the second term of Eq. (5) only terms for which $m' = m''$ survive, it is obvious that for s-p band materials, the only off-diagonal $F_{L',L''}$'s which contribute are $F_{(0,0),(1,0)}$ and $F_{(1,0),(0,0)}$, which moreover are the complex conjugates of one another.[5] [The argument is that in the set of possible L's, viz., $\{(0,0),(1,1),(1,0),(1,-1)\}$ the only different elements having the same m are $(0,0)$ and $(1,0)$.] Thus Eq. (5) may be approximated simply by

$$\Gamma(E_f, Z) \approx \sum_{L,L'} \rho_L \otimes \rho_{L'} W_{L,L,L',L'}(E_{f_1} Z) + 4\mathrm{Re}\left[\sum_L \rho_L \otimes F_{(0,0),(1,0)} \times W_{L,L,(0,0),(1,0)}(E_f Z)\right] + O(F^2_{L',L''}, L' \neq L''). \quad (8)$$

At this point there are two ways to proceed. First, we consider Auger emission in the bulk region of a solid. That is, we ignore the mean free path[6] and any Z dependence in Eq. (8), and consider the partial width for Auger emission at energy E_f, integrated over all 4π steradians of exit angle. In this limit, the quantity $B_{l_{f_1},l_{f_2},m}(E_f, Z)$ [cf. Eqs. (2.23) and (2.25) of Ref. 1] takes on the value

$$(2mE_f/\hbar^2)^{1/2} \delta_{l_{f_1},l_{f_2}}. \quad (9)$$

Thus in the "bulk" limit the l_f's in the products of matrix elements of Eqs. (6) and (7) must be equal

to one another. However, if $l_{f_1}=l_{f_2}$ and $l_1=l_1'$, and since l_i is the same in both M's, conservation of parity requires that l_2 and l_2' must either both be odd or both be even. Consequently in the "bulk" limit, we have

$$W_{L,L,(0,0),(1,0)}(E_f,Z)\to 0\,, \tag{10}$$

and thus we expect, to quadratic order in the ratio of off- to on-diagonal components of F, that

$$\Gamma^{\text{bulk}}(E_f)\approx\sum_{L,L'}\rho_L\otimes\rho_{L'}W^{\text{bulk}}_{L,L,L',L'}(E_f)\,. \tag{11}$$

Equation (11) may be evaluated straightforwardly, providing direct insight into the question of what contributes most heavily to a calculated Si $L_{2,3}VV$ Auger line shape (as well as providing a useful "reasonableness test" for a computer program). Specifically, using Eq. (9) above, as well as Eqs. (2.25) and (3.4)–(3.6) of Ref. 1 to evaluate $W^{\text{bulk}}_{L,L,L',L'}(E_f)$, we rewrite Eq. (11) in the form

$$\hbar\Gamma^{\text{bulk}}(E_f)\approx\frac{8\pi R}{3}\Big[2\mathfrak{R}_0^2(1111)\Big(\rho_p\otimes\rho_p-\frac{1}{2}\sum_m\rho_{(1,m)}\otimes\rho_{(1,m)}\Big)$$
$$+2[\mathfrak{R}_0^2(0110)+\tfrac{1}{9}\mathfrak{R}_1^2(0101)-\tfrac{1}{3}\mathfrak{R}_0(0110)\mathfrak{R}_1(0101)]\rho_s\otimes\rho_p+\tfrac{1}{3}\mathfrak{R}_1^2(1100)\rho_s\otimes\rho_s\Big], \tag{12}$$

where the $\mathfrak{R}_\kappa(l_f l_i l_1 l_2)$ are dimensionless, radial, Auger matrix elements [see Ref. 1, Eq. (3.6) for their definition], $\mathfrak{R}$ is the Rydberg, $\rho_s\equiv\rho_{(0,0)}$, and ρ_p is defined by

$$\rho_p\equiv\sum_m\rho_{(1,m)}\,. \tag{13}$$

In deriving Eq. (12) contributions involving the radial matrix elements $\mathfrak{R}_1(2101)$ and $\mathfrak{R}_2(2110)$ have been dropped because these elements are quite small in magnitude for Si (see Table I), and those involving $\mathfrak{R}_2(3111)$ and $\mathfrak{R}_2(1111)$ have been dropped because their contributions are greatly reduced by their associated angular integrals, i.e., by the factor $(2\kappa+1)^{-1}=0.2$ which [cf. Ref. 1, Eq. (3.5)] accompanies them.

In order to understand the implication of Eq. (12) roughly, let us suppose that all the $\rho_{(1,m)}$ are identical. Then $\hbar\Gamma^{\text{bulk}}(E_f)$ is given approximately as a linear combination of the self-fold of the p-like density of states, twice the cross-fold of the s- and p-like densities of states and the self-fold of the s-like DOS, locally, on a Si atom in the bulk. Consulting Table I to obtain the values of the radial matrix elements, one finds the relative weights of these three contributions to $\hbar\Gamma^{\text{bulk}}(E_f)$, to be in the approximate proportion $1:\frac{1}{2}:\frac{1}{7}$. Thus the contribution of $\rho_s\otimes\rho_s$ is greatly suppressed in $\hbar\Gamma^{\text{bulk}}(E_f)$, and that of $2\rho_s\otimes\rho_p$ somewhat reduced relative to that of $\rho_p\otimes\rho_p$. In order to obtain an $\hbar\Gamma^{\text{bulk}}(E_f)$ curve that looks more like the Auger data of Houston *et al.*,[3] one would require $\mathfrak{R}_0(111)$ to be somewhat larger and/or $\mathfrak{R}_0^2(0110)$ to be somewhat smaller, as noted above in connection with Fig. 1. However, for comparison with data it would be better to use a theoretical expression which includes surface effects.

We therefore proceed to extend our reduction of the full formula for $\Gamma(E_f,Z)$ to the case of emission from surface atoms. In this case the l_f's of the products of matrix elements in $W_{L,L,(00),(1,0)}$ are not required to be equal and thus one may not *a priori* drop the second term on the right-hand side of Eq. (8). One may still, however, take advantage of the fact that the radial matrix elements $\mathfrak{R}_1(2101)$, and those for which $\kappa=2$, contribute little to $\Gamma(E_f,Z)$. Using this fact we can write Eq. (8) more explicitly as

TABLE I. Radial matrix elements for Si $L_{2,3}VV$ Auger decays. These numbers differ from those in Ref. 1, Table II(a), because they were calculated on a finer mesh of points and also because a sign error has been corrected for the elements $\mathfrak{R}_0(0110)$, $\mathfrak{R}_1(0101)$, $\mathfrak{R}_1(2101)$, and $\mathfrak{R}_1(2101)$.

E (eV)	$\mathfrak{R}_1(1100)$	$\mathfrak{R}_0(0110)$	$\mathfrak{R}_1(0101)$	$\mathfrak{R}_1(2101)$	$\mathfrak{R}_2(2110)$	$\mathfrak{R}_2(3111)$	$\mathfrak{R}_0(1111)$	$\mathfrak{R}_2(1111)$
85	0.582×10^{-2}	0.785×10^{-2}	0.596×10^{-2}	-0.074×10^{-2}	-0.233×10^{-2}	1.046×10^{-2}	0.803×10^{-2}	0.416×10^{-2}
95	0.625	0.770	0.613	−0.038	−0.151	0.948	0.788	0.457
105	0.659	0.758	0.628	−0.016	−0.087	0.849	0.773	0.491
115	0.684	0.743	0.637	−0.006	−0.042	0.761	0.757	0.518

$$\hbar\Gamma(E_f,Z)\approx\frac{8\pi R}{3}\Bigg\{\sum_{m_1,m_2}\rho_{(1,m_1)}\otimes\rho_{(1,m_2)}\tilde{B}_{11m_2}\mathcal{R}_0^2(1111)(2-\delta_{m_1,m_2})$$
$$+2\rho_s\otimes\rho_p\tilde{B}_{000}[\mathcal{R}_0^2(0110)+\tfrac{1}{9}\mathcal{R}_1^2(0101)-\tfrac{1}{3}\mathcal{R}_0(0110)\mathcal{R}_1(0101)]+\rho_s\otimes\rho_s\Big(\frac{1}{9}\sum_{m_f}\tilde{B}_{11m_f}\Big)\mathcal{R}_1^2(1100)$$
$$+\tilde{B}_{100}\Big[\mathrm{Re}(e^{i(\varphi_1-\varphi_0)}F_{(0,0),(1,0)})\otimes\rho_s\{\tfrac{2}{3}\mathcal{R}_1(1100)[\mathcal{R}_0(0110)+\tfrac{1}{3}\mathcal{R}_1(0101)]\} \tag{14}$$
$$+\mathrm{Re}(e^{-i(\varphi_1-\varphi_0)}F_{(0,0)(1,0)})\otimes\sum_m\rho_{(1,m)}\{4\mathcal{R}_0(1111)[\mathcal{R}_0(0110)(1-\tfrac{1}{2}\delta_{m,0})+\tfrac{1}{3}\mathcal{R}_1(0101)(\delta_{m,0}-\tfrac{1}{2})]\}\Big]\Bigg\}.$$

Here the $\tilde{B}_{l_1l_2m}$ are defined by[7]

$$\tilde{B}_{l_1l_2m}\equiv\tfrac{1}{2}\Big[\frac{(2l_1+1)(2l_2+1)(l_1-m)!(l_2-m)!}{(l_1+m)!(l_2+m)!}\Big]^{1/2}\int_0^1 dx P_{l_1}^m(y(x))P_{l_2}^m(y(x))e^{-z/\lambda y(x)}, \tag{15}$$

where λ is the mean free path,[8] where

$$y(x)\equiv[(E_fx^2+V_0)/(E_f+V_0)]^{1/2}, \tag{16}$$

with V_0 equal to the inner potential, and where $P_l^m(y)$ is an associated Legendre polynomial. Also the phase φ_l is that corresponding to the large distance behavior of the lth partial wave in the final Auger electron wave function, and is defined in Eq. (3.4) of Ref. 1.

Note that in Eq. (14), the first three terms are quite similar to the three corresponding terms in Eq. (12) for $\hbar\Gamma^{\mathrm{bulk}}(E_f)$.[9] The magnitude of the last term must be evaluated numerically in order to see how reasonable it is to think of the measured $\hbar\Gamma(E)$ as being simply a linear combination of folds of the $\rho_{(l,m)}$.

The results of evaluating Eq. (14) numerically for Si(111) are shown in Fig. 3, where they are broken down into the contributions of the various $\rho_L\otimes\rho_L$, and $\rho_L\otimes F_{(0,0),(10)}$, and are also compared to the results of the full, corrected line-shape calculation. Note first that the full and approximate calculations of the $L_{2,3}VV$ Auger line shape are in excellent agreement, lending credence both to the correctness of our present computer code, as well as to the validity of the approximations underlying Eq. (14). Note also that the contributions of the folds other than $\rho_{(1,m)}\otimes\rho_{(1,m')}$ and $2\rho_s\otimes\rho_p$ are quite small and thus that the nature of the theoretical line shape is principally governed by $\mathcal{R}_0(1111)$ and by the largest matrix element involving a $3s$ and $3p$ electron, $\mathcal{R}_0(0110)$.[10] If the independent-electron theory is to describe the Si(111) $L_{2,3}VV$ Auger line shape, then, as is seen in Fig. 1, the ratio $\mathcal{R}_0(0110)/\mathcal{R}_0(1111)$ must be smaller by a factor of ~0.6 (or smaller yet, cf. Fig. 4) than its value calculated using atomic, Herman-Skillman[11] orbitals.

It must be borne in mind, however, that for an atom in the same row of the periodic table as Si, namely Ar, the Auger matrix elements calculated using Herman-Skillman orbitals lead to excellent agreement with the measured intensities of the various LMM Auger lines.[12] Thus we are faced with explaining why the location of a Si atom in a solid should lead to a significant change in the all-important quantity $\mathcal{R}_0(0110)/\mathcal{R}_0(1111)$. And to that end, we conclude this section with a brief discussion of an Auger matrix element calculation. The

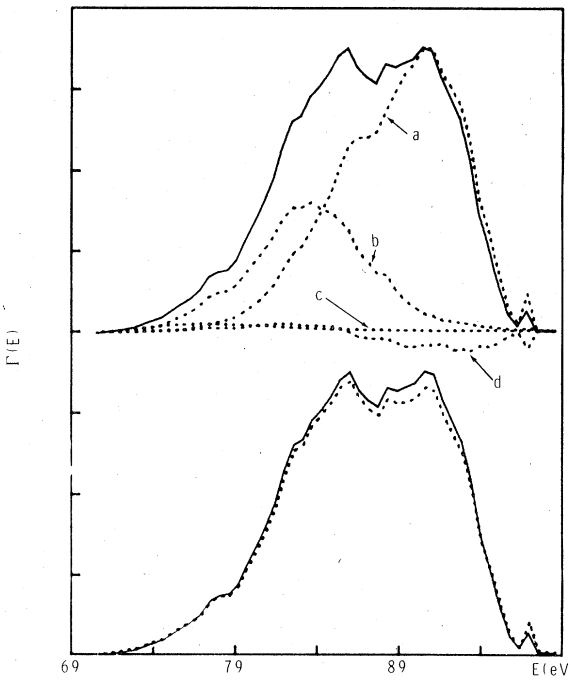

FIG. 3. Lower curves: Comparison of line shapes calculated using the simplified expression for the Si(111) $L_{2,3}VV$ transition, Eq. (14) (solid curve), and the full theory (dotted curve). Upper curves: Breakdown of contributions to the simplified model for the Auger line shapes (solid curve). Contributions due to (a) $\rho_{(p,m)}\otimes\rho_{(p,m')}$, (b) $\rho_s\otimes\rho_p$, (c) $\rho_s\otimes\rho_s$ and (d) $F_{(0,0),(1,0)}\otimes\rho_{(l,m)}$ are shown as dotted curves. For all the theoretical curves we used $\lambda=7$ Å.

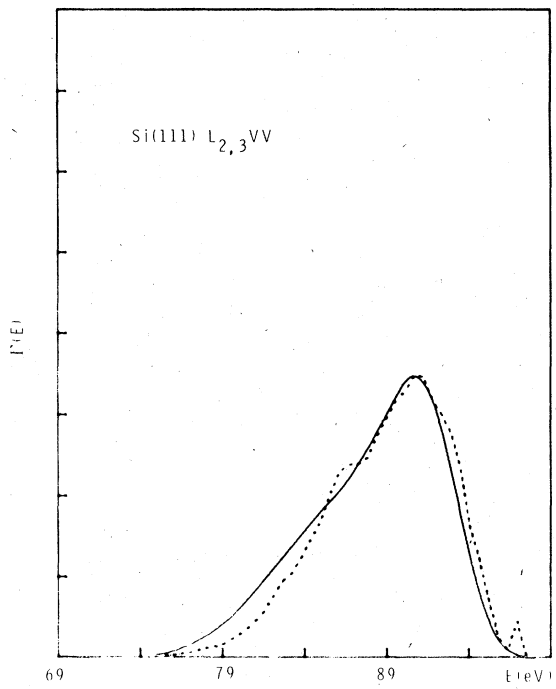

FIG. 4. Comparison of Si(111) $L_{2,3}VV$ data (solid curve), Ref. 3, with the theoretically calculated current coming only from the $\rho_{(p,m)} \otimes \rho_{(p,m')}$ terms of Eq. (14). This comparison indicates that experimentally the decay rate for processes involving other than two valence $3p$ electrons is small.

first point to note is that contributions to $\kappa = 0$ radial Auger matrix elements come strictly from the core regions of Si atoms. Specifically note [cf. Ref. 1, Eq. (3.6)] that

$$\mathcal{R}_0(l_f l_i l_1 l_2) = \int_0^\infty dr_2 \frac{F_{l_f}(p_f r_2)}{(\pi p_f)^{1/2}} \mathcal{R}_{l_2}(r_2) \times \left(\frac{1}{r_2} \int_0^{r_2} dr_1 \mathcal{R}_{l_1}(r_1) \mathcal{R}_{l_i}(r_1) + \int_{r_2}^\infty dr_1 \frac{1}{r_1} \mathcal{R}_{l_1}(r_1) \mathcal{R}_{l_i}(r_1) \right), \tag{17}$$

where $F_{l_f}(p_f r_2)/(\pi p_f)^{1/2}$ is a normalized continuum radial wave function [with $p_f = (2mE_f/\hbar^2)^{1/2}$] and where the $\mathcal{R}_l(r)$ are atomic bound-state radial wave functions. In Eq. (17) it is obvious that in the last term no contributions come from the region of space r_1 or $r_2 > a_i$, where a_i is the radius of the core orbital $\mathcal{R}_{l_i}(r)$. Moreover, since $\kappa = 0$, the orbital angular momenta of states 1 and i must be equal [i.e., $l_1 = l_i$, as is evidently the case in $\mathcal{R}_0(1111)$ and $\mathcal{R}_0(0110)$]; thus the radial wave functions $\mathcal{R}_{l_1}(r_1)$ and $\mathcal{R}_{l_i}(r_1)$ are necessarily orthogonal, and as r_2 becomes $> a_i$, the integral

$$\int_0^{r_2} dr_1 \mathcal{R}_{l_1}(r_1) \mathcal{R}_{l_i}(r_1)$$

approaches zero. Consequently the first term of Eq. (17) also only contributes for r_1 and $r_2 < a_i$.

These facts combine to imply that all contributions to the matrix elements $\mathcal{R}_0(l_f l_i l_1 l_2)$ come from within the radius of the core orbital $\mathcal{R}_{l_i}(r)$, which in the specific case of the Si $2p$ Auger decay is ~0.2 Å, compared to a nearest-neighbor distance in Si of 2.35 Å. In order to understand how the ratio $\mathcal{R}_0(0110)/\mathcal{R}_0(1111)$ is affected by the fact that a Si atom is in a solid, it is therefore necessary to ask how the valence and continuum orbitals of the Si atom are affected within 0.2 Å of the nucleus—i.e., the behavior of these wave functions in the interstitial regions is irrelevant, except insofar as it determines the wave function normalization. One possibility, suggested by this argument, is that since the atomic $3p$ orbital of Si is larger than the $3s$ orbital, the former will be more compressed when a Si atom resides in a solid, pushing up its normalization near the core. However, the wave functions used in our calculation of Auger matrix elements correspond to a Si atom which contains a $2p$ hole. Thus the $3p$ and $3s$ orbitals are already quite small compared to their sizes for neutral Si; for example ~60% of the $3p$ orbital normalization, and ~75% of that for the $3s$, is found within a sphere about the nucleus whose radius equals $\frac{1}{2}$ the bulk Si nearest-neighbor distance. Consequently the differential renormalization of the Si^+ $3s$ and $3p$ wave functions in the solid does not appear to be a large enough effect to explain the necessary decrease in the magnitude of the ratio $\mathcal{R}_0(0110)/\mathcal{R}_0(1111)$. The actual source of the observed magnitude of this ratio is thus still a matter for investigation.

$L_1L_{2,3}V$ LINES

Here again our earlier Auger line-shape theory[1] can be presented in a more transparent form. We start from the exact formula, Eq. (2.29) of Ref. 1,

$$\hbar\Gamma(E_f, Z) = 2 \sum_{L, L', m_{c'}} F_{L, L'}(E_f - E_{c'} + E_c, Z) \times W_{L_c, L_{c'}, L, L'}(E_f, Z), \tag{18}$$

where the indices c and c' refer, respectively, to the lower ($2s$) and upper ($2p$) core levels. The important feature of Eq. (18) is that W is diagonal in its first two subscripts, reflecting the fact that we must sum the partial widths for the transitions involving the $2p$ orbitals of different magnetic quantum number.[13] As a consequence, following arguments identical to those made in the previous section, one finds that m and m' in Eq. (18) must be

equal, and therefore that the only off-diagonal component of $F_{L,L'}(E,Z)$ to contribute to $\Gamma(E_f,Z)$ is $F_{(0,0),(1,0)}(E,Z)$. Thus Eq. (18) can be rewritten in the *exact* form

$$\hbar\Gamma(E_f,Z)=2\Big(\sum_{L_1 m_{c'}}\rho_L W_{L_{c'},L_{c'},L,L}(E_f,Z)+\sum_{m_{c'}}\mathrm{Re}[F_{(00),(10)}(E_f-E_{c'}+E_c,Z)\times W_{L_{c'},L_{c'},(0,0),(1,0)}(E_f,Z)]\Big), \quad (19)$$

where $\rho_L\equiv F_{LL}(E_f-E_{c'}+E_c,Z)$. We anticipate (cf. Fig. 2) that the first term in Eq. (19) will dominate, in which case the $L_1L_{2,3}V$ line shape will be approximately just a linear combination of the angular momentum projected components of the Si local state density.

The W's in Eq. (19) are easy to calculate exactly (see Appendix for the exact results). However, since for Si the radial matrix elements $\mathfrak{R}_1(201_L1_M)$ and $\mathfrak{R}_1(201_M1_L)$ are small compared to $\mathfrak{R}_1(001_L1_M)$ and $\mathfrak{R}_2(001_M,1_L)$ (cf. Ref. 1, Table II), we may ignore the former elements to lowest order, thereby finding

$$\begin{aligned}\hbar\Gamma(E_f,Z)\approx 16\pi R\Big[&\rho_s\Big(\sum_{m_f=-1}^{1}\tilde B_{1,1,m_f}\Big)[\mathfrak{R}_0^2(1001)+\tfrac{1}{9}\mathfrak{R}_1^2(1010)-\tfrac{1}{3}\mathfrak{R}_0(1001)\mathfrak{R}_1(1010)]\\&+\tfrac{1}{9}\rho_p\tilde B_{0,0,0}[\mathfrak{R}_1^2(001_L1_M)+\mathfrak{R}_1^2(001_M1_L)-\mathfrak{R}_1(001_L1_M)\mathfrak{R}_1(001_M1_L)]\\&+2\,\mathrm{Re}[e^{i(\varphi_0-\varphi_i)}F_{(0,0),(1,0)}(E_f,Z)]\tilde B_{1,0,0}[\tfrac{1}{3}\mathfrak{R}_0(1001)\mathfrak{R}_1(001_M1_L)\\&+\tfrac{1}{9}\mathfrak{R}_1(1010)\mathfrak{R}_1(001_L1_M)-\tfrac{1}{6}\mathfrak{R}_0(1001)\mathfrak{R}_1(001_L1_M)-\tfrac{1}{18}\mathfrak{R}_1(1010)\mathfrak{R}_1(001_M1_L)]\Big].\end{aligned} \quad (20)$$

By virtue of the definitions of the $\tilde B_{l_1,l_2,m}$ and of the $P_l^m(y)$ it is clear that

$$3\tilde B_{000}\equiv\sum_{m_f=-1}^{1}\tilde B_{1,1,m_f}. \quad (21)$$

Thus to the extent that the last term of Eq. (20) is small, we have

$$\begin{aligned}\hbar\Gamma(E_f,Z)\approx 16\pi R\tilde B_{0,0,0}\{&\rho_s[3\mathfrak{R}_0^2(1001)+\tfrac{1}{3}\mathfrak{R}_1^2(1010)-\mathfrak{R}_0(1001)\mathfrak{R}_1(1010)]\\&+\tfrac{1}{9}\rho_p[\mathfrak{R}_1^2(001_L1_M)+\mathfrak{R}_1^2(001_M1_L)-\mathfrak{R}_1(001_L1_M)\mathfrak{R}_1(001_M1_L)]\}.\end{aligned} \quad (22)$$

Looking back at Fig. 2, one notes that $|F_{(0,0),(1,0)}(E_f,Z)|$ is quite small for the Si(111) 1×1 surface except at the energy of the dangling bond (where substantial mixing of s-like and $l=1$, $m=0$ orbitals is necessary to produce the directionality of that bond). Thus, except at the dangling bond energy, the neglect of the last term of Eq. (20) turns out to be accurate to within a few percent. At the dangling bond energy the error incurred by neglecting the $F_{(0,0),(1,0)}$ contribution in Eq. (20) is more like 30%. However since there is little evidence that on a real Si(111) surface a dangling bond state exists in the gap, it is reasonable to ignore the quantitative inaccuracy of Eq. (22) at the dangling bond energy.

If one thus assumes the validity of Eq. (22), a reasonable procedure to follow in analyzing Si(111) $L_1L_{2,3}V$ Auger line-shape data is to attempt to fit the experimental line shape with a linear combination of the calculated partial densities of states, thereby determining the ratio

$$\frac{3\mathfrak{R}_0^2(1001)+\tfrac{1}{3}\mathfrak{R}_1^2(1010)-\mathfrak{R}_0(1001)\mathfrak{R}_1(1010)}{\tfrac{1}{9}[\mathfrak{R}_1^2(001_L1_M)+\mathfrak{R}_1^2(001_M1_L)-\mathfrak{R}_1(001_L1_M)\mathfrak{R}_1(001_M1_L)]}. \quad (23)$$

It is then for the theorist to explain the experimental value of this quantity.

In the upper panel of Fig. 5, a comparison of Si(111) $L_1L_{2,3}V$ data[3] is shown with theoretical curves actually calculated using the full formula for $\hbar\Gamma(E_f,Z)$, Eq. (19) [which as explained is little different from what one obtains using Eq. (22)], and folded with a Lorentzian of width 0.8 eV to account roughly for the lifetime broadening of the Si $2s$ state.[2] The matrix elements $\mathfrak{R}_0(1001)$ and $\mathfrak{R}_1(1010)$ in the theoretical curve have each been reduced by a factor, 1/2.5, from their atomically calculated values in order to make the highest and lowest energy peaks in the theory agree in relative intensity with the data. As was discussed in Ref. 1, at present one does not know what physics is responsible for this large reduction in the matrix elements for $3s$ electrons. And moreover, we do not understand at present, why the experimental curve is as broad as it is. Note in the lower panel of Fig. 5 that if the theoretical curve is folded with a Lorentzian of 2-eV width, then the agreement between theory and experiment is excellent, apart from the fact that the middle experimental peak corresponds to a slight dip in the theoretical curve.

Similar results are shown for the Si(001) 1×1

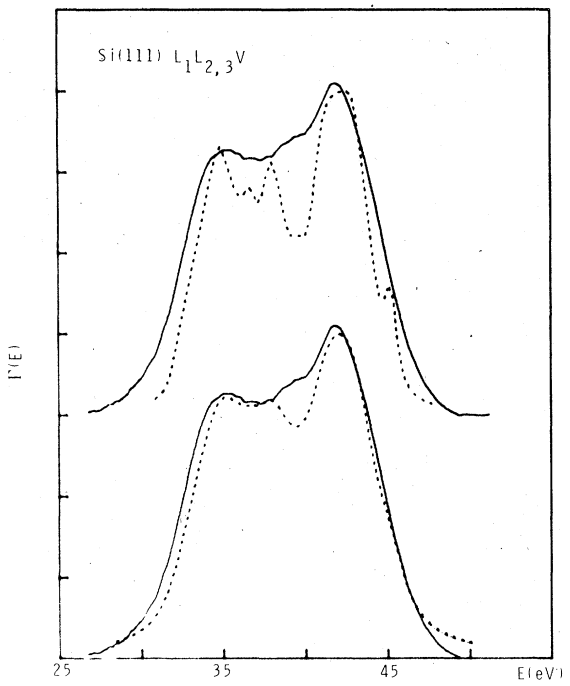

FIG. 5. Comparison of data (Ref. 3) for the Si(111) $L_1L_{2,3}V$ line (solid curve), and theory (dotted curve). In the upper theoretical curve the calculated results were folded with a Lorentzian of width 0.8 eV. In the lower panel we used a Lorentzian width of 2.0 eV. In both cases λ was taken to be 7 Å, and the matrix elements involving 3*s* electrons are reduced by the factor 1/2.5. Essentially no shift of the theoretical energy scale was required to bring the theoretical and experimental curves into alignment, contrary to what was reported in Figs. 7–9 in Ref. 1.

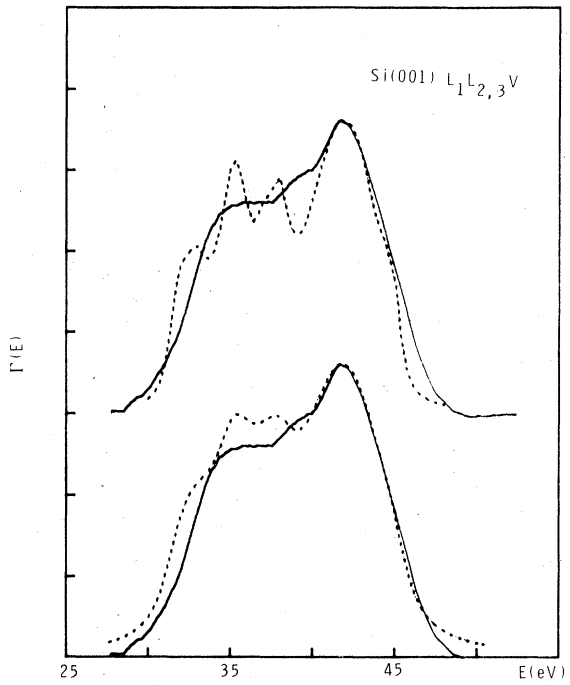

FIG. 6. Comparison of data (Ref. 3) for the Si(001) $L_1L_{2,3}V$ line (solid curve) and theory for an unreconstructed Si(001) $1\times_1$ surface (dotted curve). The upper and lower theoretical curves correspond to folding with Lorentzians of widths 0.8 eV and 2.0 eV, respectively. The matrix elements for transitions involving 3*s* electrons have been reduced here by the factor 1/2.5. The mean free path was taken to be 7 Å.

surface in Fig. 6. In this case the use of a theoretical density of states based on an unreconstructed surface leads to worse agreement with experiment than in the (111) case. Specifically, there is no evidence in the experimental curves for either split off back-bonding states on the low-energy side of the $L_1L_{2,3}V$ data or for a dangling bond state on the high energy side.

Finally, it should be pointed out that the theory curves in Figs. 5 and 6 incorporate corrections of a number of minor computer code errors in our earlier work,[1] which were found through the use of Eq. (20) as a consistency check. Also the statement made in the figure caption of Figs. 7–9 of Ref. 1, to the effect that a 3-eV shift of the theory curves was necessary to align them with the data, was incorrect. Within the uncertainty of the experimental energy scale, no shift of the theory was necessary at all.

CONCLUSIONS

The fact that the off-diagonal components of the occupied local density-of-states matrix can generally be expected to be small permits one to write simplified expressions for Auger line shapes in terms of the angular momentum components of the ordinary LDOS. As a consequence it is found to be relatively easy to parametrize Auger lineshape data in such a way as to provide the theorist with values of Auger matrix elements and with hole widths to try to understand. At present the confrontation of theory and experiment for the Si $L_1L_{2,3}V$ and $L_{2,3}VV$ lines produces a number of problems. Specifically for both these cases we must learn why matrix elements involving emission of 3*s* electrons are smaller experimentally than they are when calculated using atomic orbitals. Also we need to understand why the $L_1L_{2,3}V$ lines are a volt or so broader than one would expect on the basis of x-ray photoelectron spectroscopy measurements of 2*s* hole widths in the third row of the periodic table.[2]

APPENDIX

We present here the exact formula for the shape of an $L_1L_{2,3}V$ line in an s-p band material. The formula is

$$\begin{aligned}\hbar\Gamma(E_{f_1}Z) = 16\pi R\Bigg(&\sum_{m_f=-1}^{1}\tilde{B}_{11m_f}[\mathcal{R}_0^2(1001)+\tfrac{1}{9}\mathcal{R}_1(1010)-\tfrac{1}{3}\mathcal{R}_0(1001)\mathcal{R}_1(1010)]\rho_s\\
&+\tfrac{1}{9}\tilde{B}_{000}[\mathcal{R}_1^2(001_L1_M)+\mathcal{R}_1^2(001_M1_L)-\mathcal{R}_1(001_L1_M)\mathcal{R}_1(001_M1_L)]\rho_p\\
&+\tfrac{1}{45}[\mathcal{R}_1^2(201_L1_M)+\mathcal{R}_1^2(201_M1_L)-\mathcal{R}_1(201_L1_M)\mathcal{R}_1(201_M1_L)]\\
&\times[(\rho_{(1,1)}+\rho_{(1,-1)})(6\tilde{B}_{222}+3\tilde{B}_{221}+\tilde{B}_{220})+\rho_{(1,0)}(6\tilde{B}_{221}+4\tilde{B}_{220})]\\
&+\frac{2}{9\sqrt{5}}\cos(\varphi_2-\varphi_0)\tilde{B}_{200}[\mathcal{R}_1(201_L1_M)\mathcal{R}_1(001_L1_M)+\mathcal{R}_1(201_M1_L)\mathcal{R}_1(001_M1_L)\\
&\qquad-\tfrac{1}{2}\mathcal{R}_1(201_M1_L)\mathcal{R}_1(001_L1_M)-\tfrac{1}{2}\mathcal{R}_1(201_L1_M)\mathcal{R}_1(001_M1_L)]\\
&\times(2\rho_{(1,0)}-\rho_{(1,1)}-\rho_{(1,-1)})+2\,\mathrm{Re}[e^{i(\varphi_0-\varphi_1)}F_{(0,0)(1,0)}(E_f,Z)]\tilde{B}_{100}\\
&\times[\tfrac{1}{3}\mathcal{R}_0(1001)\mathcal{R}_1(001_M1_L)+\tfrac{1}{9}\mathcal{R}_1(1010)\mathcal{R}_1(001_L1_M)-\tfrac{1}{6}\mathcal{R}_0(1001)\\
&\quad\times\mathcal{R}_1(001_L1_M)-\tfrac{1}{18}\mathcal{R}_1(1010)\mathcal{R}_1(001_M1_L)]\\
&+2\,\mathrm{Re}(e^{i(\varphi_2-\varphi_1)}F_{(0,0)(1,0)})\Big(2\sqrt{\tfrac{3}{5}}\tilde{B}_{1,2,0}+\frac{2}{\sqrt{5}}\tilde{B}_{121}\Big)\\
&+[\tfrac{1}{3}\mathcal{R}_0(1001)\mathcal{R}_1(201_M1_L)+\tfrac{1}{9}\mathcal{R}_1(1010)\mathcal{R}_1(201_L1_M)-\tfrac{1}{6}\mathcal{R}_0(1001)\mathcal{R}_1(201_L1_M)-\tfrac{1}{18}\mathcal{R}_1(1010)\mathcal{R}_1(201_M1_L)]\Bigg).\end{aligned}$$

For an $L_{2,3}VV$ transition in an s-p band material the exact expression contains too many terms to make writing out the full expression practical.

---

*Work prepared for the U. S. ERDA under Contract No. AT(29-1)-789.

[1]P. J. Feibelman, E. J. McGuire, and K. C. Pandey, Phys. Rev. B 15, 2202 (1977).

[2]The widths of the $2s$ levels in Na, Mg, and Al are found in x-ray photoelectron spectroscopy to be 0.28 ± 0.033 eV, 0.45 ± 0.02 eV, and 0.75 ± 0.05 eV, respectively [P. H. Citrin (private communcation)].

[3]J. E. Houston, M. G. Lagally, and G. Moore, Solid State Commun. 21, 879 (1977).

[4]We use the notation $\Gamma(E,Z)$ here for an Auger partial width rather than $R^2J(E)$ as in Ref. 1.

[5]Reference 1, Eq. (2.16).

[6]In other words, we set the mean free path equal to ∞.

[7]Cf. Ref. 1, Eq. (2.23).

[8]In Ref. 1, the quantity $\frac{1}{2}\lambda$ was used in Eq. (15) rather than λ. Thus λ in Ref. 1 was twice the mean free path. Here λ is the mean free path itself.

[9]The geometric factors $\tilde{B}_{l_1,l_2,m}$ in Eq. (14) have little effect on the relative weights of transitions involving two $3p$ electrons and one $3s$ and one $3p$ electron. This fact follows since it can easily be shown using the properties of associated Legendre polynomials that $\tilde{B}_{111}+\tilde{B}_{110}+\tilde{B}_{11-1}\equiv3\tilde{B}_{000}$.

[10]$\mathcal{R}_1(0101)$ contributes less because everywhere it appears it is accompanied by the factor $\frac{1}{3}$, i.e., $(2\kappa+1)^{-1}$ with $\kappa=1$.

[11]F. Herman and S. Skillman, *Atomic Structure Calculations* (Prentice-Hall, Englewood Cliffs, N.J., 1963).

[12]E. J. McGuire, Phys. Rev. A 11, 1880 (1975).

[13]In other words, amplitudes for transitions involving different m_c, do not interfere; this result remains true if the core-level c' is spin-orbit split, as long as the deep core level c, is not and neither are the valence band states.

[14]The notations 1_L1_M mean p states from the L and M shells, respectively.